A nonlinear approach to the wind strength of Gothic Cathedrals: the case of Notre Dame of Paris

Paolo Vannucci, Filippo Masi, Ioannis Stefanou

A nonlinear approach to the wind strength of Gothic Cathedrals: the case of Notre Dame of Paris

P. Vannucci*[1], F. Masi[2], and I. Stefanou[2]

[1]LMV, Laboratoire de Mathématiques de Versailles - UMR8100, CNRS & UVSQ.
University Paris-Saclay, Versailles (F)

[2]Laboratoire Navier - UMR8205, CNRS, ENPC & IFSTTAR.
Université Paris-Est, Marne La Vallée (F)

January 7, 2019

https://doi.org/10.1016/j.engstruct.2019.01.030

Abstract

The problem of assessing the strength to wind actions of Gothic Cathedrals is addressed in this paper. A nonlinear approach, based upon a large-strain, large displacements formulation and using a nonlinear constitutive law modeling the no-tension behavior of the material as a damage law is proposed. The method is applied to the study of the Cathedral Notre Dame of Paris.

Key words: Wind actions, Gothic Cathedrals, nonlinear FEM, Notre Dame of Paris

1 Introduction

Gothic Cathedrals are one of the most important cultural heritages of Europe. They characterize the panorama of several European towns and prove the skill and boldness of the architects of the Middle Ages. Though unaware of the laws of physics, they conceived audacious buildings that defy the laws of mechanics since eight centuries.

As very imposing and articulated stone structures, Gothic Cathedrals have been the object of some studies, aiming at understanding, on one hand, the way these structures have been conceived and, on the other hand, how much safe they are, namely with respect to the self weight loads and the wind thrust.

*Corresponding author: Paolo Vannucci. LMV, 45 Avenue des Etats-Unis. 78035 Versailles, France
E-mail: paolo.vannucci@uvsq.fr

Rather surprisingly, there are few studies on this last problem; without going back to old treatises, like [Ungewitter, 1890], treating classically the problem of lateral forces using the method of the thrust line, a fundamental work has been that of R. Mark. In his book *Experiments in Gothic Structure*, he tackles the analysis of the lateral wind forces on a Gothic Cathedral using the experimental technique of photoelasticity, [Mark, 1982].

It is interesting to notice that R. Mark investigated, with this technique, the response of Notre Dame of Paris as built before the structural modifications made after 1225. The motivation of his study is in his own words:

> *This relatively lightly constructed central vessel of the Cathedral Notre Dame is thirty-three meters from floor to vault keystone, a full eight meters taller than its highest Gothic predecessors, the Cathedrals of Laon and Sens, and the largest single-incremental height increase for a new church over an earlier building in the entire era. Since wind speeds are greater at higher elevations, and wind pressure is proportional to the square of the speed, earlier experience with lower-profiled, more heavily massed churches could not have fully prepared the builders to cope with the new environment. Because of massive reconstructions made to Notre Dame after 1225, just how the design problem was solved in the original Gothic construction remained unclear* [Mark, 1984].

His objective was hence to understand if the modifications made by the architects of the XIII-th century were motivated by some structural reasons, and not exclusively by architectural and stylistic ones. In particular, R. Mark has shown that the original structure, with a different arrangement of the flying buttresses, had some structural problems. Namely, he showed that under the wind action of heavy storms, tensile stresses exceeding three to five times the tensile admissible stresses for the mortars of the Middle Ages arose in some part of the structure, so certainly producing evident cracks. This can explain, in the opinion of R. Mark, why the structure was modified after 1225. The present structure of the Cathedral is shown in Fig. 1, while the original one is presented in Fig. 2; the structural differences, mainly concerning the flying buttresses, are evident.

R. Mark made experiences with photoelasticity also on other Cathedrals, namely Amiens and Beauvais, [Mark, 1982]. However, it is worth recalling that the underlying assumption of photoelasticity is the linearly elastic behavior of the structure, assumption that can be considered as correct only for analyses that are restrained to situations where there are not significative cracks arising in the structure. This exactly happens when the structure approaches its ultimate state under extreme winds. So, such an approach for the determination of the ultimate wind strength of a Cathedral can be questionable.

A more recent work is that of M. Como and his team, [Como, 2013], [Coccia et al., 2015]. In a research concerning the Amiens Cathedral, the study of the lateral wind strength is done using the limit analysis method, i.e. calculating the ultimate load multiplier λ_{cr} of the wind pressures over the lateral parts of the Cathedral. For $\lambda = \lambda_{cr}$, the structure is transformed into a mechanism by the formation of a sufficient number of plastic hinges, rotation points formed by the cracking of the stone masonry under the action of tensile stresses. The theoretical framework is that defined by Heyman, [Heyman, 1995], i.e., the masonry has no tensile strength at all, the compressive strength can be considered as infinite and no sliding failures occur in the structure. Actually, in [Coccia et al., 2015] also local sliding mechanisms are anyway considered.

The study is conducted on a planar scheme, obtained considering a transversal portion of the Cathedral between two successive pillars of the main aisle. The two analyses make use of slightly different hypotheses for the calculation of the wind pressure, which finally results in two different values of the ultimate wind speed at 10 m above the ground, which passes from 146 km/h in the first study to 109 km/h in the second one.

Such wind speed values have been exceeded in France rather frequently, also during recent extreme events: a velocity of 220 km/h has been recorded at Cap Finistère, in Bretagne, on October 15, 1987. During the storms of December 26 and 28, 1999, a wind speed of 169 km/h has been measured at Parc Montsouris, inside the city of Paris, while during the storm Xynthia, February 28, 2010, the wind has reached the speed of 136 km/h at Metz, well far from the coasts. Very recently, on January 12, 2017, the storm Egon has produced wind gusts at 146 km/h at Dieppe and has destroyed the rose of the Cathedral of Soissons.

These few data show that extreme wind storms, potentially able to produce important structural damages and possibly the ruin of tall buildings, are rather frequent. Such events are to be considered with care today, because climate deregulation produced by global warming has rendered the occurrence of extreme meteorological events more frequent than in the past. So, the structural analyses of important historical buildings like Gothic Cathedrals, more sensitive to such events due to their dimensions and type of structure, are more and more important.

To this purpose, we have studied the response to a lateral wind of the Cathedral Notre Dame of Paris, with the intention of determining its ultimate strength: our goal was *to give an assessment of the critical wind, the one able to produce the global failure of the structure*. We have followed a different approach with respect to the studies cited above. In particular, we performed an incremental analysis in order to determine the response of the structure, in terms of horizontal displacements, to different wind velocities. When the displacements, increased by increasing wind loads, become unbounded, failure occurs.

This choice has been inspired by three considerations: on one hand, to perform a limit analysis on a five-aisles Cathedral with galleries is much more cumbersome than the same analysis on a Cathedral of the High Gothic period, like that of Amiens, with only three aisles and no galleries, [Jantzen, 1957], [Simson, 1962], [Frankl, 1963], [Wilson, 1990]. To determine all the possible failure mechanisms for such a kind of structure is very delicate.

On the other hand, the incremental approach that we have used allows us to find, for each wind speed, the equilibrium configuration. In this way, the progressive damage of the structure appears automatically and the precise failure mechanism arises spontaneously from the nonlinear numerical simulation.

Finally, unlike other previous studies, our approach makes use of a 3D structural scheme. Actually, the use of a 2D simplified structural scheme for the prediction of the wind strength of building as complex as a Gothic Cathedral remains questionable: the simplifications that are done in the passage from the 3D structure to a 2D scheme are numerous and strong and could affect the results. In our approach we make use of a 3D model representing a significative part of the Cathedral's structure, that we have called the

structural unit, described below. Through this approach the structural failure mechanism is automatically detected as a result of the calculation, which is an advantage with respect to customary limit analysis 2D approaches, where strong simplifications on the geometry and a-priori assumptions on the failure mechanisms are done (see Sect. 6.2).

Finally, the deformation of the structure is determined for each incremental value of the wind action, so letting appear the time response of the Cathedral to wind. However, because we do a quasi-static analysis, where all dynamical effects are neglected, the time so considered is a synthetic one, a purely numerical quantity that cannot be transformed into a physical time. Nonetheless, by this procedure we can draw curves simulating the time response of the Cathedral.

As already mentioned, all the simulations have been done on a finite element model of a *structural unit* of the main aisle, specified below. The simulations are non-linear, because of the constitutive equation, a softening law representing the tensile damage of the material, used to model the no-tension behavior of stone masonry (material nonlinearity), and because we have performed the calculations considering large deformations and displacements (geometric nonlinearity), that occur when the structure is close to its ultimate state.

This paper is organized as follows: in Sect. 2 we introduce the structure of the Cathedral Notre Dame of Paris and its finite element model. In Sect. 3 we detail the constitutive law used to model the material and in Sect. 4 the representation of the wind loads. The details about the numerical procedure and simulations are given in Sects. 5 and 6.1, while some final considerations are presented in Sect. 7.

2 The structural model

The Cathedral Notre Dame of Paris, one of the principal examples of the Early Gothic period, was built from 1163 and during about one century. Its overall dimensions are: length 130 m, width 48 m, height of the vaults 32.5 m, total height, comprehending the timber roof, 45 m. The high vault of the main aisle is built with a sexpartite scheme, i.e. each vault is composed by six webs. The scheme of the structure is shown in Fig. 1. The Cathedral has five aisles plus the lateral chapels and wide galleries that, above the lateral aisles, run all along the principal aisle and round the choir.

The geometry of Notre Dame of Paris is hence particularly complex and articulated, much more than other Cathedrals of the High Gothic period, like Chartres, Reims or Amiens, where galleries are not present and the aisles are only three. Also the dimensions are different: though when it was built it was the highest Cathedral, for the race to height typical of Gothic architecture it soon was exceeded in height by other Cathedrals. So, because it is less high than other major Cathedrals, like Amiens or Beauvais, the transversal section of Notre Dame of Paris is stiffer and stronger compared to them. A sketch of the historical evolution of the height of French Gothic Cathedrals is given in Fig. 2.

For this study, we have considered a *structural unit*, which is the part of the Cathedral shadowed in Fig. 1. It comprehends a complete sexpartite vault, 12 m in length, and

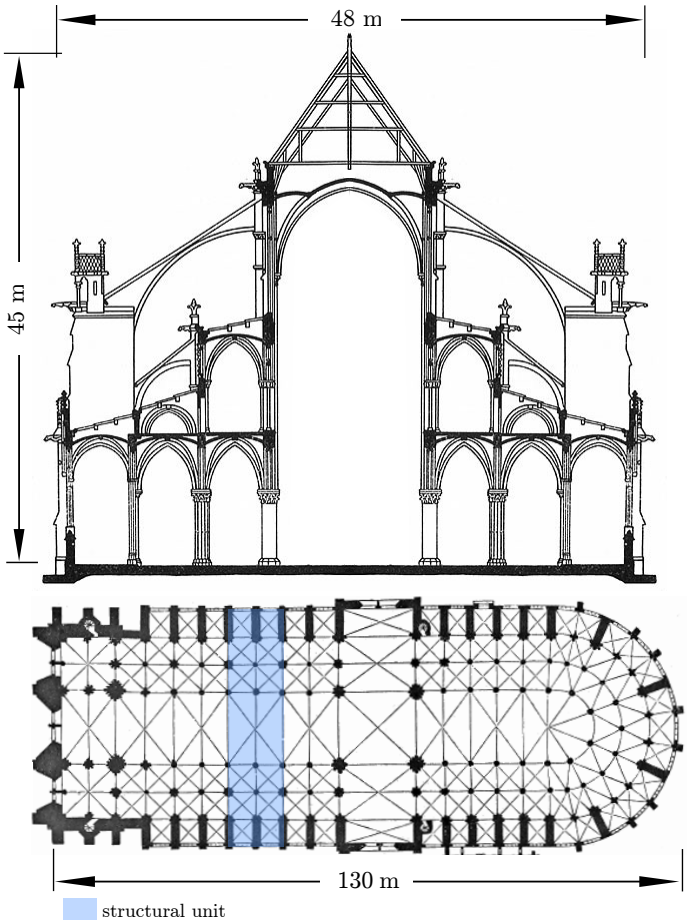

Figure 1: The Cathedral of Notre-Dame in Paris: section (top) and plan view (bottom), after the reconstruction started in 1225 and the restoration of Viollet-le-Duc, in the XIX-th century.

the entire width of the Cathedral. A detailed numerical model has hence been done, represented in Figs. 3 to 5, based upon a survey of the Cathedral and the laserscan survey done by A. Tallon, of Vassar College, [Tallon, 2010].

Due to the complexity of the Gothic architecture, some geometrical simplifications, not affecting the overall structural response of the Cathedral, have been done. In particular, all the parts that are merely decorative are not taken into account – e.g., crockets, windows, traceries and pinnacles. The ribbed vaults are modeled carefully, together with the pointed arches and the flying buttresses, since the stability and integrity of the whole building depend on them. Also, the filling in the springing zone of the vaults have been modeled until an angle of 30° on the horizontal, see Fig. 5.

In order to avoid a meaningless growth of the finite element model, the roof of the building has been modeled just to take on the wind actions. So, it is represented by two rigid inclined plates whose top is 10 m above the guttering walls, like in the Cathedral. The roof, made of lead and wood, applies an estimated linear load of 2×10^4 N/m on the top of each one of the guttering walls. All the simulations have been done using the finite element code ABAQUS.

Taking advantage of its symmetry, calculations are made just on one half of the *structural*

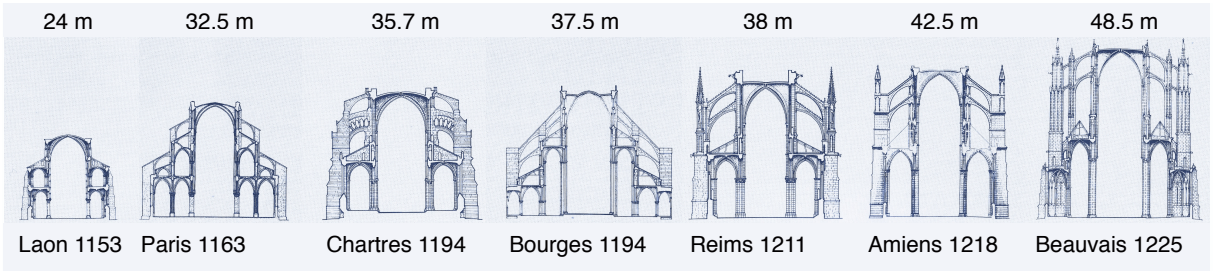

Figure 2: Historical evolution of the Gothic Cathedrals height (from [Mark, 1984]).

Figure 3: The numerical model of Notre Dame of Paris: overall view.

unit, i.e., a portion of the Cathedral of 6 m in length, indicated in blue in Fig. 6. In the same figure, we have indicated the boundary conditions: all the nodes at the base of columns and walls, i.e. belonging to plane π_1, are completely blocked: $u_x = u_y = u_z = 0$, with $\mathbf{u}= (u_x, u_y, u_z)$ the displacement vector, while for the points in the two vertical planes π_2 and π_3 only the longitudinal displacement is constrained, $u_x = 0$.

The finite element discretization used in the simulations consists of tetrahedral elements, supported by both the standard and explicit solvers of ABAQUS, with an average element size of 0.2 m, in which *ad-hoc* refinements are pursued in some parts, due to the complexity of the geometry. The fineness of the mesh has been chosen after an accurate convergence analysis, performed in order to obtain a reliable degree of accuracy with an acceptable length of the computing time. The details about the convergence analysis are given in Appendix A. In consideration of the convergence analysis results, we have selected a finite element model with $\sim 1.83 \times 10^6$ elements for a total size of the model of $\sim 1.25 \times 10^6$ degrees of freedom. Details of the mesh used in the simulations are shown in Fig. 7.

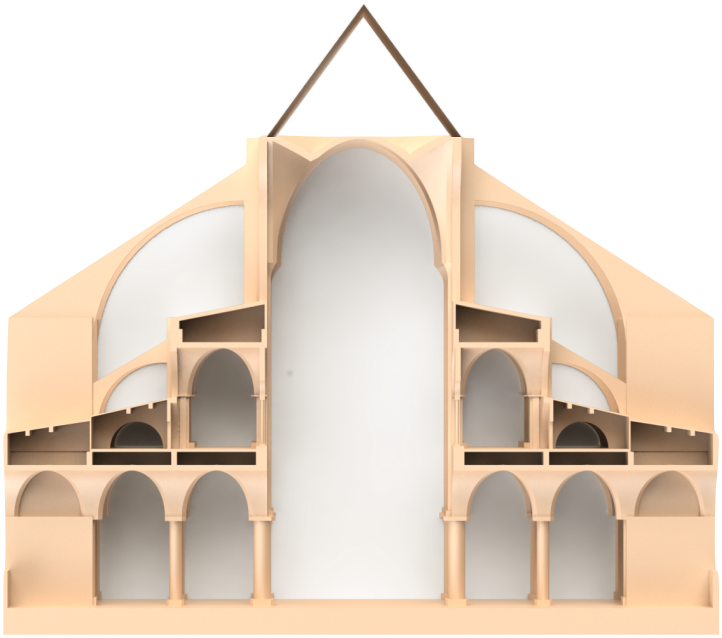

Figure 4: The numerical model of Notre Dame of Paris: transversal section.

3 The material model

Masonry composed by ashlars and mortar joints is often modeled as a no-tension material: its tensile strength is so small that in some cases it can be considered as practically null, while the compressive strength is so high, usually greater than 40 MPa, that it is never attained in the body of the structure (normally, the highest compression in monumental structures is of the order of $4 \div 6$ MPa).

Hence, a suitable constitutive law must be used to model a continuum composed of ashlars and mortar-joints. Such a law should model the possibility of damage of the material, i.e. the formation of cracks due to tensile stresses. In our calculations, the following assumptions have been made to model the nonlinear behavior of stone structures:

- in compression, the material is described by an isotropic linearly elastic constitutive law with infinite strength. This is a strong assumption, [Heyman, 1995], [Stefanou et al., 2015], but it is not expected to alter the results (as said above, compressions are always far below the admissible compressive stress);
- in tension, the material is assumed to be isotropic linearly elastic until the maximum principal stress does not exceed the tensile strength; a small, but not null, tensile strength f_t is hence considered for the material;
- when the maximum principal stress exceeds the tensile strength f_t, failure is modeled using a nonlinear constitutive law based on the softening model proposed by Hillerborg, Modéer and Petersson, [Hillerborg et al., 1976].

The Cathedral Notre Dame of Paris is built with ashlars of a limestone extracted from quarries of the Paris region. Not all the stones are from the same quarry, hence the mechanical characteristics of the material are not uniform throughout all the building. In addition, no certain data are available about the mechanical properties of the stone

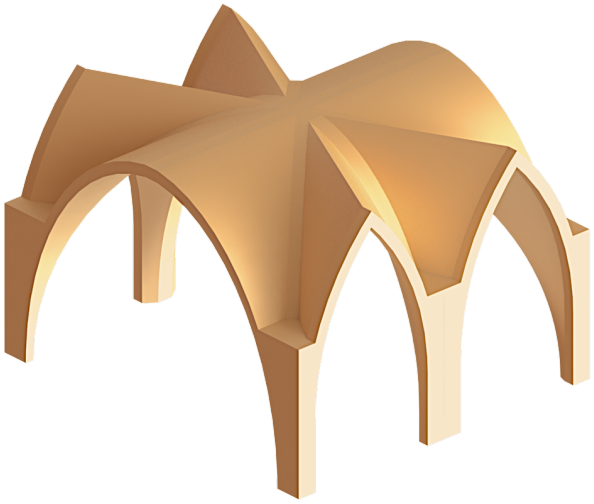

Figure 5: The numerical model of Notre Dame of Paris: the sexpartite vault.

and of the mortar used by the constructors. Moreover, the cathedral has undergone several renovations over the centuries, the most important one being that of Viollet Le Duc during the XIXth century. That is why it is today completely impossible to know in detail the mechanical characteristics of all the materials composing the Cathedral, nor their distribution and an average value of the different mechanical characteristics has to be used. That is why data derived from the literature have been used for the simulations.

An equivalent homogenized Young's modulus E_{eq}, assuming that both stone and mortar-joints have the same Poisson's ratio, is derived from classical homogenization theory, see e.g. [Cecchi and Sab, 2002], [Como, 2013], namely

$$E_{eq} = \frac{E_m\,(1 + s/h_b)}{E_m/E_b + s/h_b}, \tag{1}$$

where E_b and E_m are the Young's moduli respectively of masonry blocks and mortar-joints, while h_b and s are the height of the blocks and thickness of the joints. Relying on the investigations made during a survey of the building, we can evaluate $h_b = 2.5 \times 10^{-1}$ m and $s = 1.0 \times 10^{-2}$ m. For the mortar, a modulus $E_m = 2.5$ GPa is chosen, while for the stone a modulus $E_b = 20$ GPa is selected, which is a mean value for limestone (for more details, see again [Como, 2013]). The resulting Young's modulus is $E_{eq} = 14.8$ GPa, and finally a value $E_{eq} = 14$ GPa is selected, for a matter of safety. The Poisson's ratio and the density are selected relying on typical values mentioned in the literature for limestone, namely:

$$\rho_s = 2000 \text{ kg/m}^3, \qquad \nu_s = 0.25.$$

In the softening model that we have used to represent the formation of cracks, [Hillerborg et al., 1976], when f_t, the maximum allowed tensile strength, is exceeded, damage occurs and the subsequent tensile softening is characterized in terms of the fracture energy G_f, i.e., the energy dissipated during the opening of a unit area of crack in Mode I.

We introduce a bilinear approximation of the softening curve, represented in Fig. 8. Following this approximation, we can compute the fracture energy for normal tensile

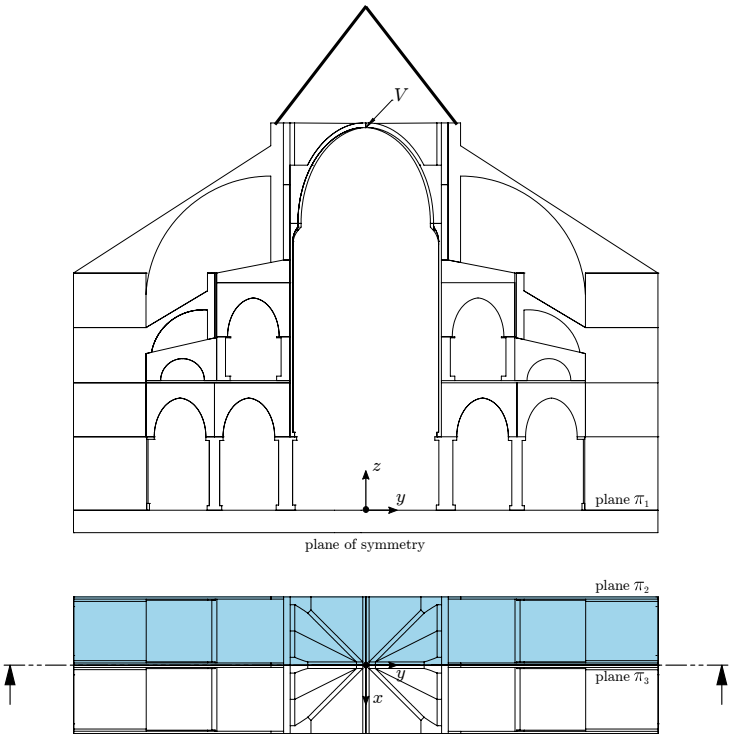

Figure 6: The part of the unit studied (highlighted in blue).

stresses as

$$G_f = G_f^1 + G_f^2 = \int_0^{w_k} \sigma \, dw + \int_{w_k}^{w_f} \sigma \, dw, \tag{2}$$

where σ is the maximum principal stress; w is the displacement normal to the crack surface; w_k is the normal displacement relative to the kink point, with stress σ_k, and w_f the one corresponding to the complete loss of strength. Applying the bilinear approximation in terms of the following parameters,

$$\Psi = \frac{\sigma_k}{f_t}, \quad \lambda = \frac{w_k}{w_f}, \tag{3}$$

the two integrals in eq. (2) become

$$\begin{aligned} G_f^1 &= \int_0^{w_k} \sigma \, dw = \frac{f_t}{2} \lambda \left(1 + \Psi\right) w_f, \\ G_f^2 &= \int_{w_k}^{w_f} \sigma \, dw = \frac{f_t}{2} \Psi \left(1 - \lambda\right) w_f, \end{aligned} \tag{4}$$

so that

$$G_f = \frac{f_t}{2} \left(\lambda + \Psi\right) w_f. \tag{5}$$

This expression allows to compute w_f if G_f, f_t, Ψ and λ are known:

$$w_f = \frac{2}{\Psi + \lambda} \frac{G_f}{f_t}. \tag{6}$$

For masonry, relying on the experimental results from uniaxial tensile tests on specimens with a characteristic length $h = 100$ mm, [van der Pluijm, 1999], the following parameters

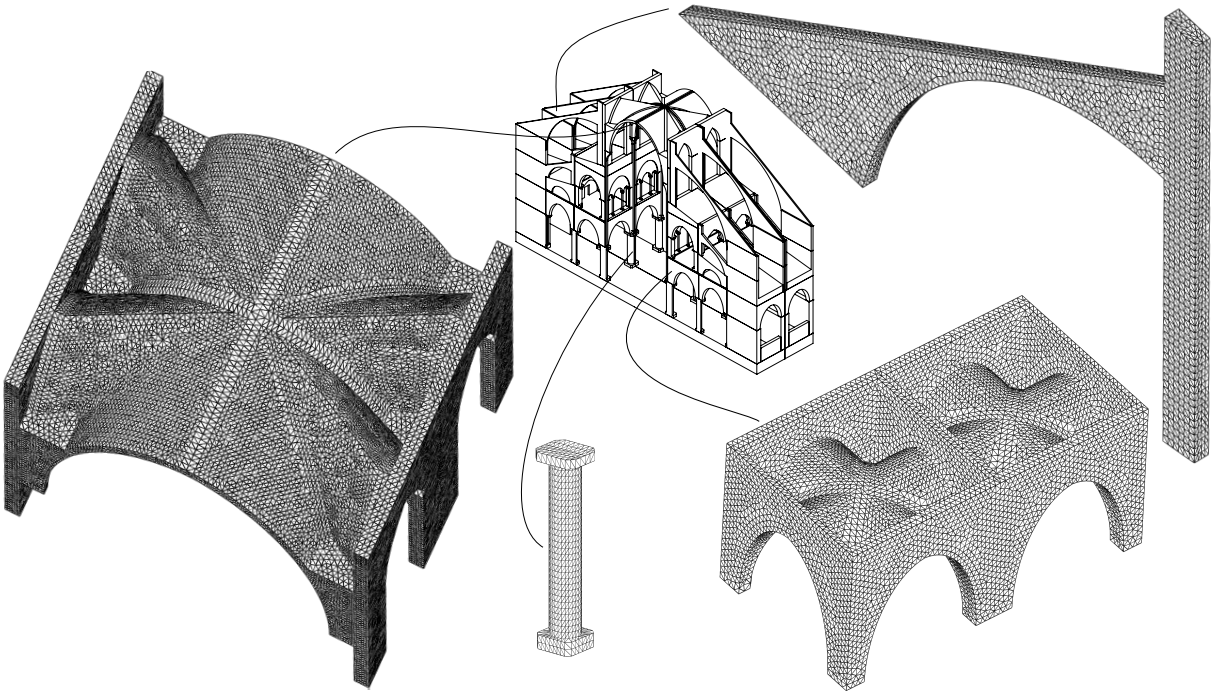

Figure 7: Details of the mesh used for the finite element analyses.

have been chosen

$$f_t = 0.5 \text{ MPa}, \qquad G_f = 11.3 \text{ N/m}, \qquad \Psi = \frac{1}{3}, \qquad \lambda = \frac{1}{2}.$$

The value of w_f is automatically calculated for each element by *ABAQUS*; for instance, for $h = 100$ mm we get $w_f = 5.4 \times 10^{-2}$ mm.

4 The wind model

As said in the Introduction, we are interested in assessing the highest wind speed that the Cathedral can withstand before a global structural failure. To this purpose, we need a model of the wind as close as possible to the real physical phenomenon, in order to reproduce, as finely as possible, a realistic situation.

The wind close to the Earth surface is just what happens in the boundary layer of the flow of air masses. As such, we need a law describing the *wind profile*, i.e. the variation of the wind speed v with the distance z from the ground, typical of what happens in a boundary layer: a null speed at $z = 0$ and a decreasing gradient $dv(z)/dz$.

Different models simulate the wind profile; typical ones are logarithmic or power laws, [Sachs, 1978]. Like in an analogous work on the wind strength of a Gothic Cathedral, [Coccia et al., 2015], we have used a power law in the form

$$\eta = \zeta^{\alpha}, \tag{7}$$

where we have introduced the two dimensionless variables

$$\eta = \frac{v}{v_0}, \quad \zeta = \frac{z}{z_0}, \tag{8}$$

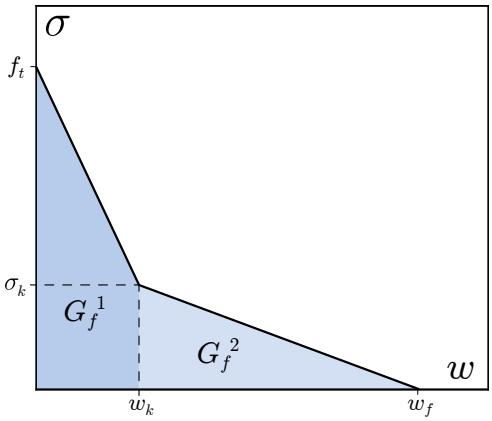

Figure 8: Traction-separation diagram and fracture energy.

with z_0 the reference height, where the wind speed v_0 is known, and α an exponent, put equal to 0.35 in [Coccia et al., 2015], value suggested for urban areas.

Actually, the wind speed is not exactly null at the ground level and, mainly for the ruggedness of the surface, it is practically constant until a certain height. Putting such a height equal to z_0, the wind profile is modified accordingly: below $z_0, v = v_0$, above, $v(z)$ is given by eq. (7). A similar scheme is used also in the norm Eurocode 1, [ECS, 2005], where however a logarithmic law is preferred. In Appendix B we give a comparison of the wind profile (7) with that proposed by Eurocode 1, showing that actually the differences between the two models are not substantial. Considering the skyline of Paris, we have chosen for z_0 the value of 10 m. The same value is suggested by Eurocode 1; finally, the wind profile is depicted in Fig. 9.

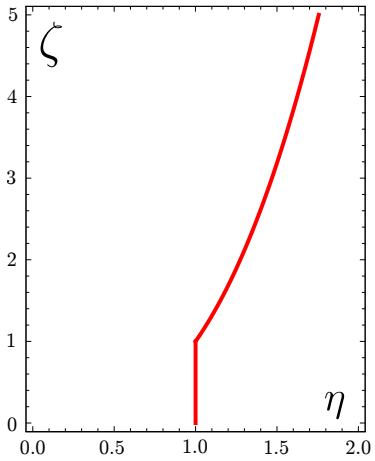

Figure 9: Wind speed profile ($\alpha = 0.35$).

The wind pressure p is obtained as a drag force per unit of exposed surface using the relation

$$p = \frac{1}{2} C_D \, \rho \, v^2, \tag{9}$$

where ρ is the mass density of air, $\rho = 1.225$ kg/m^3 at an ambient temperature of 15°C, and C_D is the drag coefficient. Its value mainly depends upon the Reynolds number, the

form and exposition of the surface impinged by wind, besides its ruggedness and other parameters, like the Mach and Froude numbers etc.

In the case of a so complex structure like the Cathedral Notre Dame, a global value for C_D could be obtained uniquely by preliminary tests in a wind tunnel. Because this has not been possible, we have evaluated C_D following some indications that can be found in the literature. In particular, cf. [Sachs, 1978], for an infinitely long rectangular plate set on the ground, $C_D \sim 1.2$; the global dimensions of the Cathedral of Paris are: height $z_1 = 45$ m at the roof top and overall length 130 m, so with a ratio length/height of ~ 3. In order to take into account for, on one hand, the *macrosopic* ruggedness of the surface, full of pinacles, statues, decorations, flying buttresses etc., and, on the other hand, of the finiteness of the side wall (for instance, for a plate into a 3D flow, $C_D = 1.28$), we have prudently increased the value of C_D and we have assumed $C_D = 1.5$. To this purpose, we remark that in [Coccia et al., 2015] the evaluation given for the wind pressure corresponds to put, on the whole, $C_D = 1.5$, and that $C_D = 1.5$ is practically the global value suggested, *in fine*, also by Eurocode 1 (see Appendix B).

R. Mark proposed in [Mark, 1982] the distribution of C_D in Fig. 10. It has been derived by experimental measures in wind-tunnel tests conducted at the Universities of Iowa, [Chien et al., 1951], and of Toronto, [Davenport, 1967], though not specifically on geometries like those typical of a Gothic Cathedral. Such a distribution shows that the overall value of C_D can considerably vary, and it attains average values ranging from ~ 1.2 to ~ 1.8.

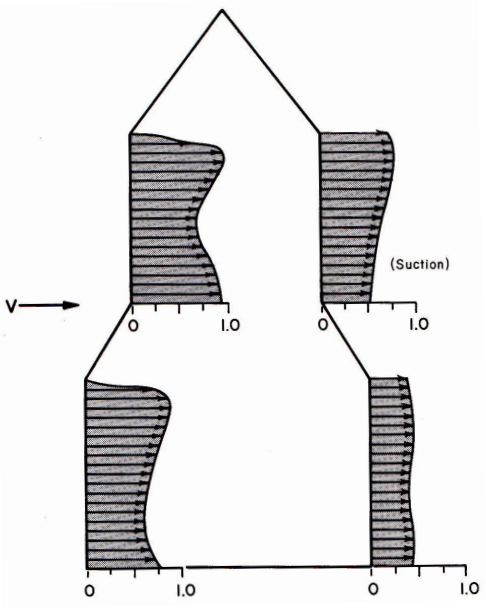

Figure 10: Distribution of C_D on a Gothic-Gathedral, according to [Mark, 1982].

It is worth to give the pressure distribution (9) in a dimensionless form. To this end, let us introduce the pressure p_0, corresponding to the value of the wind speed v_0:

$$p_0 = \frac{1}{2} C_D \, \rho \, v_0^2. \tag{10}$$

Then, the dimensionless value π of the pressure is obtained as

$$\pi = \frac{p}{p_0} = \begin{cases} 1 & \text{if } \zeta \leq 1, \\ \eta^2 = \zeta^{2\alpha} & \text{if } \zeta > 1. \end{cases} \tag{11}$$

The function $\pi(\zeta)$ is represented in Fig. 11. It is apparent that for $\zeta > 1$, i.e. for $z > z_0$, $\pi(\zeta)$ is almost linear.

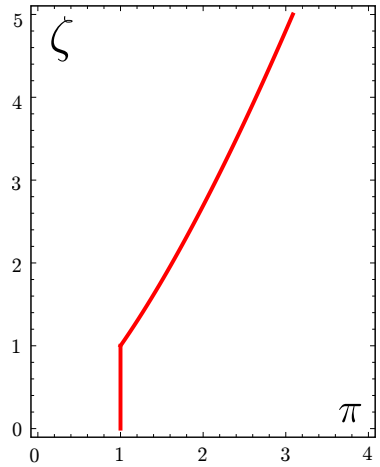

Figure 11: Wind pressure profile.

The value of p corresponds to the overall wind thrust on the Cathedral, per unit of area. Nevertheless, this action is distributed partly on the windward side and partly on the leeward side. Considering the experimental diagram of C_D in Fig. 10 and following what done in [Como, 2013] and [Coccia et al., 2015], we consider a leeward side (suction) load which is half of the windward one, i.e.

$$p = p_w + p_\ell, \quad p_w = 2p_\ell \;\Rightarrow\; p_w = \frac{2}{3}p, \quad p_\ell = \frac{1}{3}p, \tag{12}$$

where p_w indicates the windward pressure load and p_ℓ the leeward one. In Fig. 12 we give the scheme of the wind loading on the Cathedral.

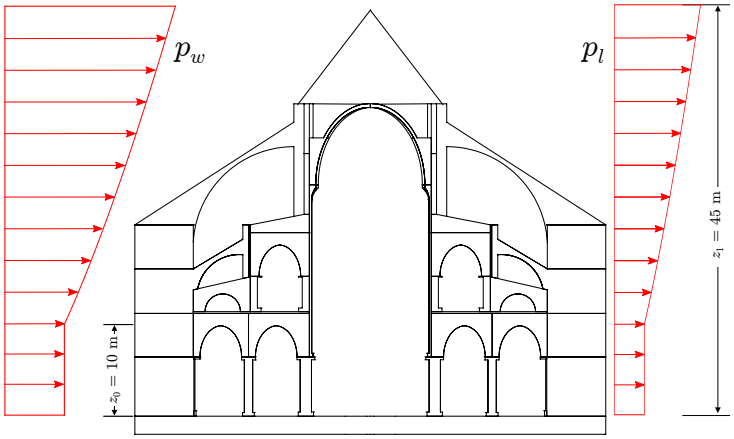

Figure 12: Wind loading on the Cathedral.

5 The method for the calculation of the wind strength

The basic idea for the evaluation of the wind strength of the Cathedral is to control the horizontal displacement of the upper part of the Cathedral. For a given value of the wind pressure, such a displacement is calculated. The wind strength of the Cathedral is then identified with the wind speed that produces an unbounded displacement of the keystone of the high vault, indicated by point V in Fig. 6.

In fact, because the constitutive law is nonlinear and it describes also the damage produced by tensile stresses, the structure of the Cathedral will have a nonlinear response to wind and a damage will appear for a sufficiently great value of the wind pressure. Such a damage, cracks propagating into the structure, will increase with the wind pressure, until a point where it will be so extended throughout the structure that a ruin mechanism will be formed. At that point, the structure will not be anymore able to withstand the wind loads and the displacement of V will progress indefinitely with time, i.e. it will be unbounded.

To take into account for the stress distribution produced by the self weight of the Cathedral, an implicit static analysis is previously done. The resulting configuration is then used as the starting point for a subsequent nonlinear explicit analysis, in which the wind loads described in Sect. 4 are applied in a quasi-static manner. A fictitious mass proportional damping is assumed in order to reach equilibrium rapidly and to dissipate unwanted oscillations (quasi-static condition).

As mentioned above, the simulations are done applying the load smoothly in time. The value of the wind pressure $p(z)$ is multiplied by a factor $A(t)$ that varies from $A_0 = 0$, for $t = t_0$, to $A_f = 1$, for $t \geq t_f$. Different choices are possible to have a smooth variation of $A(t)$, we have put

$$A(t_n) = \begin{cases} A_0 + (A_f - A_0)\, t_n^3 \left(10 - 15t_n + 6t_n^2\right) & \text{if } 0 \leq t_n < 1, \\ 1 \quad \text{if } t_n \geq 1, \end{cases} \tag{13}$$

where

$$t_n = \frac{t - t_0}{t_f - t_0}. \tag{14}$$

The diagram of $A(t_n)$ is shown in Fig. 13. For $t_n \geq 1$, the load conserves indefinitely the same maximum value.

The incremental analysis allows to obtain the response curve of the structure, i.e. the curve displacement of V versus time, for any value of the wind speed. When the structure reaches an equilibrium configuration under the applied wind pressure, the response curve shows an horizontal asymptote, indicating that the horizontal displacement has come to a value that remains constant under the wind action. On the contrary, when the Cathedral reaches its ultimate state, the response curve diverges, due to the fact that the structure has failed: cracks have formed a collapse mechanism and the horizontal displacement becomes unbounded.

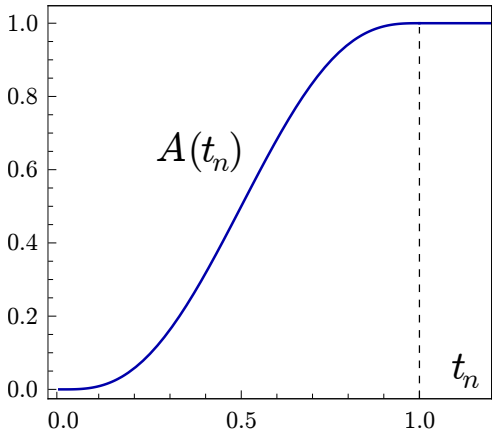

Figure 13: The diagram of factor $A(t_n)$.

6 Structural analyses

6.1 Evaluation of the critical wind speed

We have executed structural analyses for different wind speeds. In all the cases, the wind speed taken as reference is v_0, i.e. the speed at $z_0 = 10$ m above the ground level. In Tab. 1 we give, as functions of v_0, the corresponding values of p_0, p_{max} and v_{max}, where the maximum values are, of course, those corresponding at $z = 45$ m.

Table 1: Wind speeds at $z_0 = 10$ m, corresponding wind pressures min and max and wind speeds at $z = 45$ m.

v_0 [km/h]	v_{max} [km/h]	p_0 [kPa]	p_{max} [kPa]
74	125.1	0.40	1.1
92	156.4	0.62	1.8
111	187.7	0.89	2.5
129	219.0	1.21	3.5
148	250.3	1.58	4.5
166	281.6	2.00	5.7
185	312.8	2.47	7.1
203	344.1	2.99	8.6
222	375.4	3.56	10.2

For each wind speed, we have hence searched the non-linear response of the Cathedral, in terms of horizontal displacement of point V. Once the critical pressure p_0^{crit} found, i.e. the pressure p_0 leading to a global ruine of the cathedral, through eq. (10) we obtain v_0^{crit}, i.e. the critical wind speed, conventionally measured at $z_0 = 10$ m above the ground level, that the Cathedral can withstand.

The results of the calculations are shown in Figs. 14 to 16 and in Tab. 2. It is evident from these diagrams that $v_0^{crit} = 222$ km/h. In fact, for this wind speed the diagram of the displacement diverges with time: the displacement increases with the duration of the

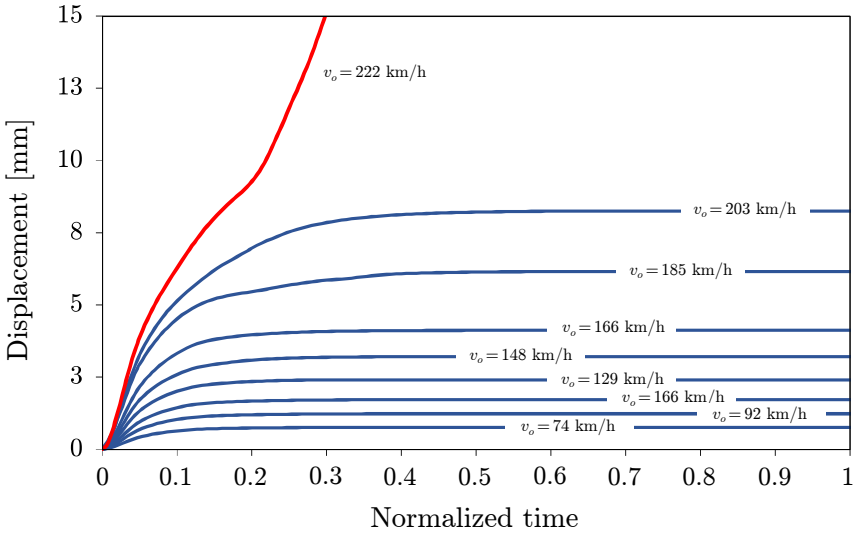

Figure 14: Diagrams time-displacement for various wind speeds v_0.

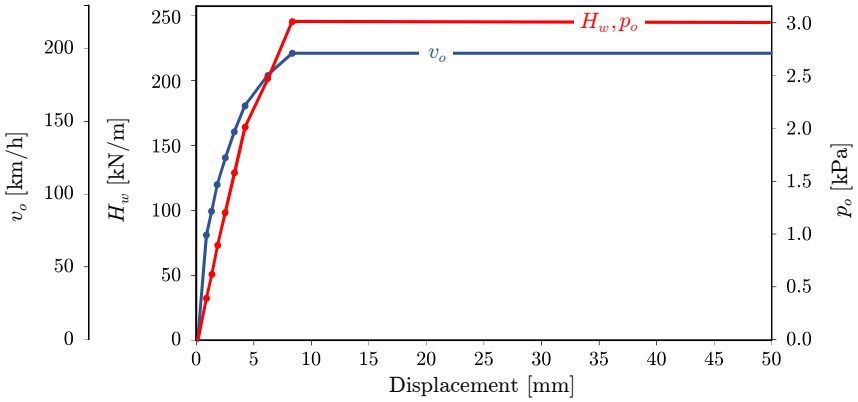

Figure 15: Wind speed, v_0, total horizontal wind thrust per unit length, H_w, and wind pressure, p_0, versus the horizontal displacement of point V, δV_{max}.

simulation. This is the sign that the structure has been transformed into a mechanism by the propagation of the cracks.

The maximum wind speed, at the roof top, corresponding to v_0^{crit} is of about 375 km/h, cf. Tab. 1. Such a meteorological event is very improbable: the highest wind speed ever recorded in France is just of 360 km/h, on November 1^{st} 1968, at the top of Mont Aigoual, at 1567 m above the sea level, much more than 45 m. This means that the structural collapse of Notre Dame of Paris as the consequence of a wind storm is a very unlikely event.

In Tab. 2, we show, for each wind speed, δV_{max}, the maximum horizontal displacement of point V, along with the overall horizontal wind thrust per unit length, H_w. We have indicated the ultimate displacement as ∞, because for the critical wind speed δV_{max} is unbounded.

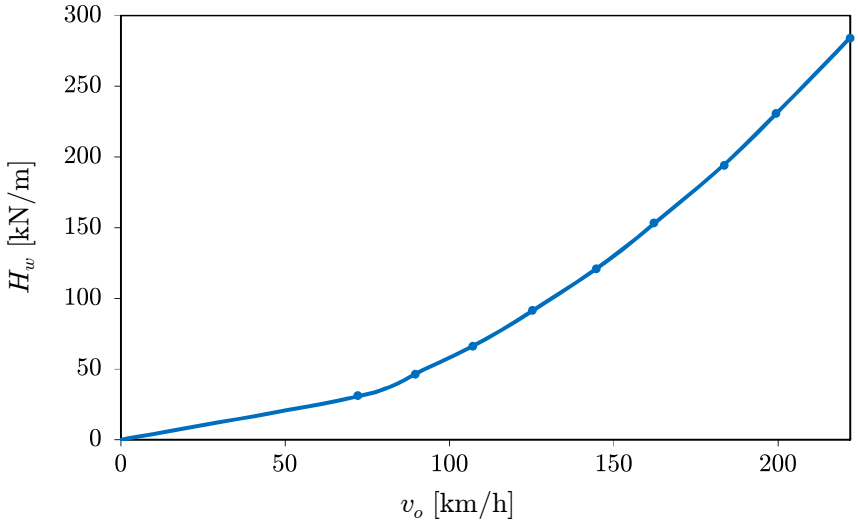

Figure 16: Total horizontal wind thrust per unit length H_w versus the horizontal displacement v_0.

Table 2: Horizontal displacements δV_{max} of point V and total wind thrust per unit length H_w versus v_0.

v_0 [km/h]	δV_{max} [mm]	H_w [kN/m]
74	0.76	31.612
92	1.23	49.394
111	1.72	71.128
129	2.41	96.813
148	3.21	126.450
166	4.12	160.038
185	6.16	197.578
203	8.25	239.069
222	∞	284.512

6.2 The mechanism of structural collapse

The numerical simulations described above allow to follow the diffusion of the damage in the structure, which leads to the formation, for the critical wind speed v_0^{crit}, of the collapse mechanism. At this stage, in fact, the damage is so extended to form a mechanism, leading to the failure of the structure, as already explained.

The phases of the structural collapse are shown in Fig. 17 and in Fig. 18, where, for the sake of comprehension, the magnitude of the lateral displacement is mapped onto the Cathedral structure through a color code. For different wind speeds v_0, the deformation of the structure and the propagation of the cracks are clearly visible. For better understanding the sequence of damages leading to the Cathedral's failure, the formation of the critical zones, eventually leading to the global failure of the structure, is indicated in Fig. 19 on the curve relating the wind speed to the horizontal displacement of point V.

As it was to be expected, the failure occurs when the flying buttresses are severely damaged by the wind thrust; the clearstorey can then rotate after the formation of four *plastic hinges*, produced by the propagation of cracks, in the high vault and at the base of the same clearstorey. The cracks propagating, also the massive buttresses are damaged and collapse. Large cracks appear also in the vaults of the lateral aisles. It is worth noting that the final mechanism leading to the global failure comprehends some plastic hinges, i.e. zones where the rotation is highly concentrated, due to the formation of cracks, as well as some sliding zones, i.e. parts where the cracks that are formed become separation/sliding surfaces, namely in the buttresses, and also separation of parts under tension. This fact confirms the results found in [Coccia et al., 2015]: failure mechanisms not purely *à la Heyman* can exist.

It is interesting to highlight the collapse of the high sexpartite vault, depicted in Fig. 20. The plastic hinges on the vault deserve a particular consideration: they are more or less longitudinal, though they are not produced over a cylindrical surface, like a barrel vault, but on a sexpartite ribbed vault. So, the location of the plastic hinges in the vault is confirmed, by a 3D model, to be similar to that often used in a 2D scheme, see [Coccia et al., 2015] again. However, the results obtained by the 3D simulation show something more: the formation of a plastic hinge corresponds still to a restricted zone severely damaged by the formation of cracks, but we can see now that the propagation of the cracks happens not only through the thickness of the section, but it interests a complex structure, like a sexpartite vault, far from being a simple rectangular cross section. This produces, for instance, a propagation of the cracks not only through the thickness of the vault, but also along its longitudinal axis: cracks do not appear simultaneously all along the vault. This 3D approach allows hence to better understand the mechanics of the global collapse of the Cathedral than in the case of a 2D simplified scheme. In addition, we are able to follow step by step the extension of the damage throughout the structure.

Comparing the results in Fig. 18 with those in Sect. 8.4 of [Como, 2013], we can see the difference between the failure mechanisms of the Cathedrals of Paris, with 5 naves, and that of Amiens, a typical 3-naves church. Unlike in the case of Amiens, where the collapse is supposed to interest the building from the foundations, in the case of the Cathedral of Paris the global collapse concerns mainly the upper part, tribunes and clearstorey, and the failure of the flying buttresses, much longer than those of Amiens, plays a fundamental role in the structural failure.

The total estimated weight of the Cathedral unit, highlighted in red in Fig. 1, is $W_{tot} \sim$ 60300 kN; so the ratio with the horizontal wind thrust that causes the structural collapse is

$$\frac{W_{tot}}{H_w} = \frac{60300}{284.512 \times 12} \sim 17.66,$$

a value which is not so far from the ratio, 18.7, calculated by R. Mark for Amiens, [Mark, 1982]. This difference is, probably, mostly due to the height of the Amiens Cathedral, 54 m, greater than that of Paris, 45 m: a lesser wind thrust is likely to produce the structural failure in that case.

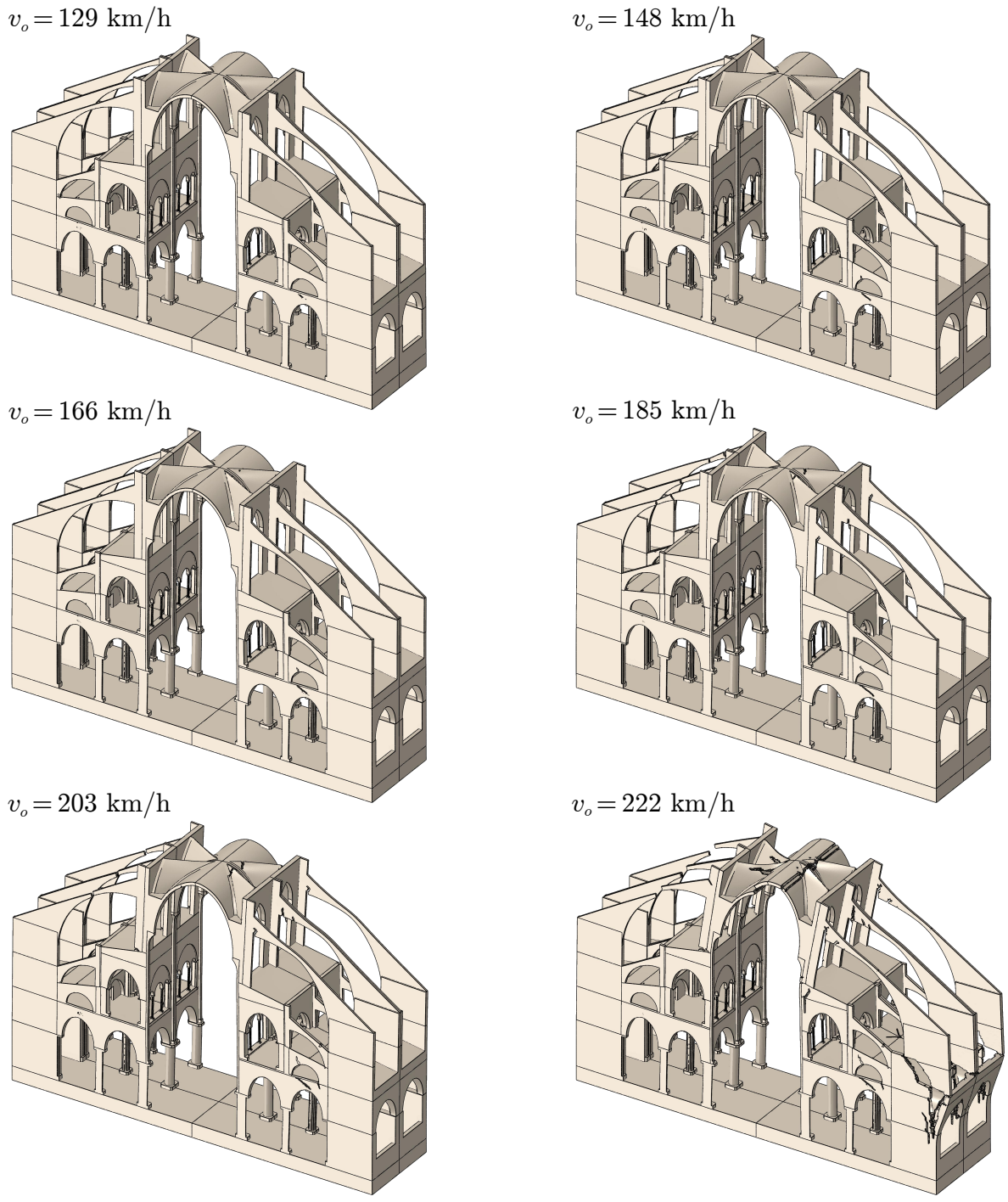

Figure 17: Progressive damage of the structure and formation of the collapse mechanism.

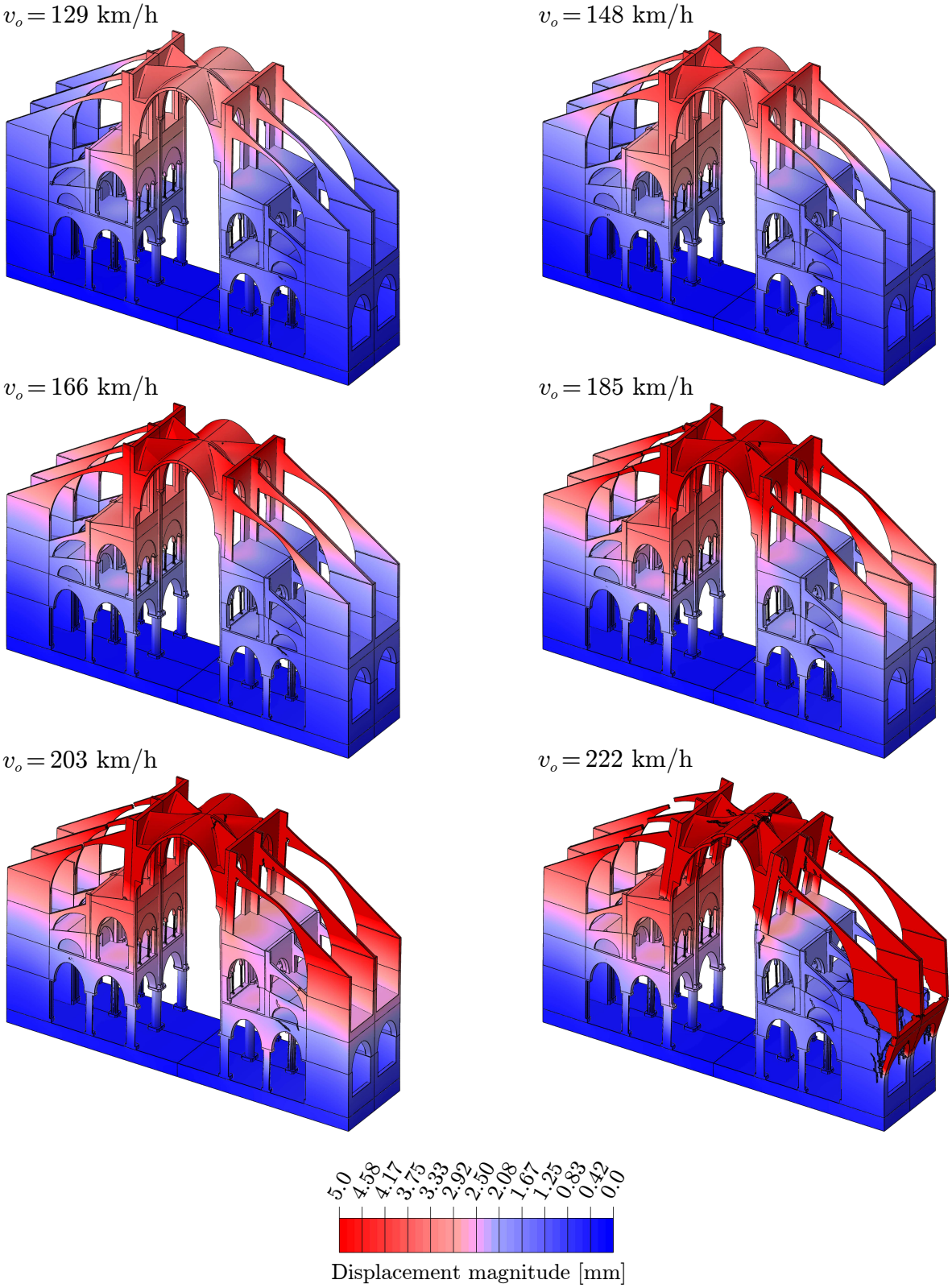

Figure 18: Progressive damage of the structure with color chart of the horizontal displacements.

Finally, it is worth noting that, though the wind speed v_{0crit} is highly improbable, since $v_0 \sim 148$ km/h a damage appears in the structure, see Fig. 17, in the form of cracks. Hence, though the global structural failure of the Cathedral under the action of the wind is unlikely to happen, winds that can produce non negligible damages to the Cathedral are really possible. As said in the Introduction, in December 1999, a wind speed of 169 km/h has been recorded inside Paris.

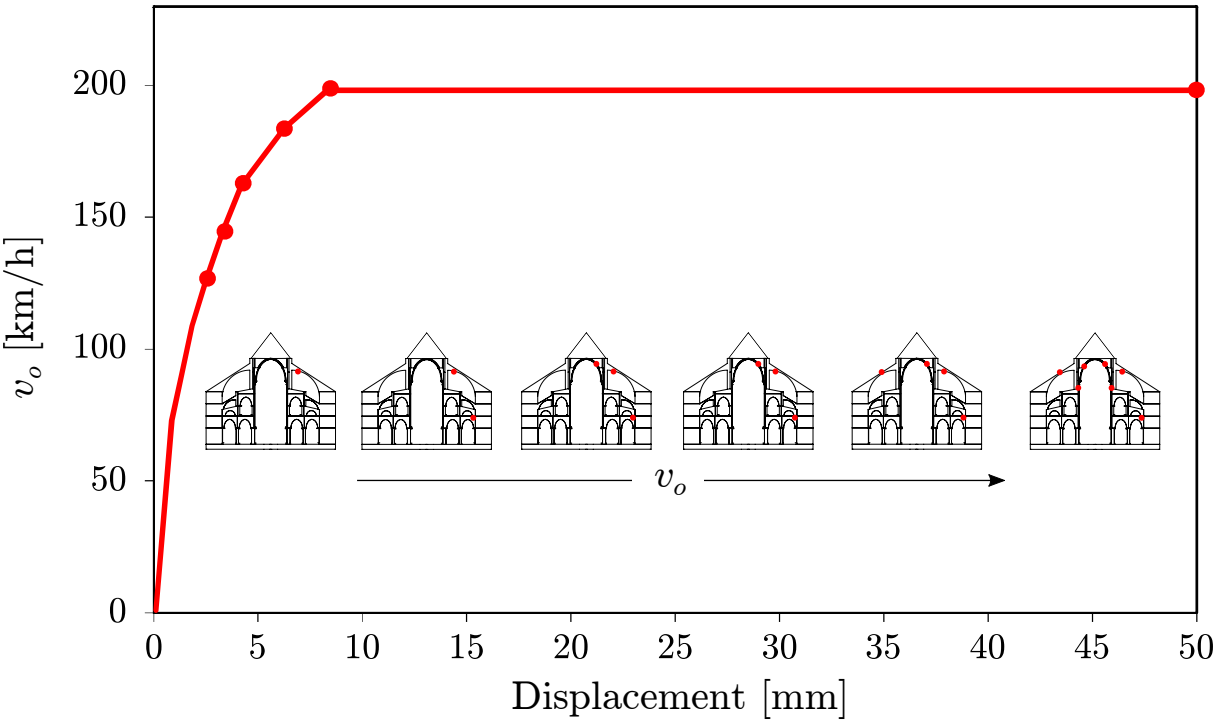

Figure 19: The failure sequence of the Cathedral; the dots on the Cathedral sections indicate the formation of a severe damage, leading to a plastic hinge or a sliding zone.

7 Conclusion

The numerical simulations have clearly shown that severe wind storms are able to damage the structure of the Cathedral Notre Dame of Paris, but that a global structural failure is highly improbable.

Of course, we have just considered in this study the global collapse of the Cathedral. However, partial, though important, local damages can be produced in different parts of the Cathedral, like the pinacles, the timber spire, the roses, the flying buttresses, the same timber roof. It is not excluded that local important effects can be produced by phenomena like vortex shedding, while the roof could be lifted up or overthrown by the wind.

All these phenomena, that could happen also for wind speeds $v_0 < v_0^{crit}$, should be studied apart and cannot be predicted with the approach followed in this paper, conceived to determine the overall strength to wind thrust and that has however different advantages. Namely, it allows to follow the progressive failure of the structure under increasing wind speed and also to determine its true collapse mechanism.

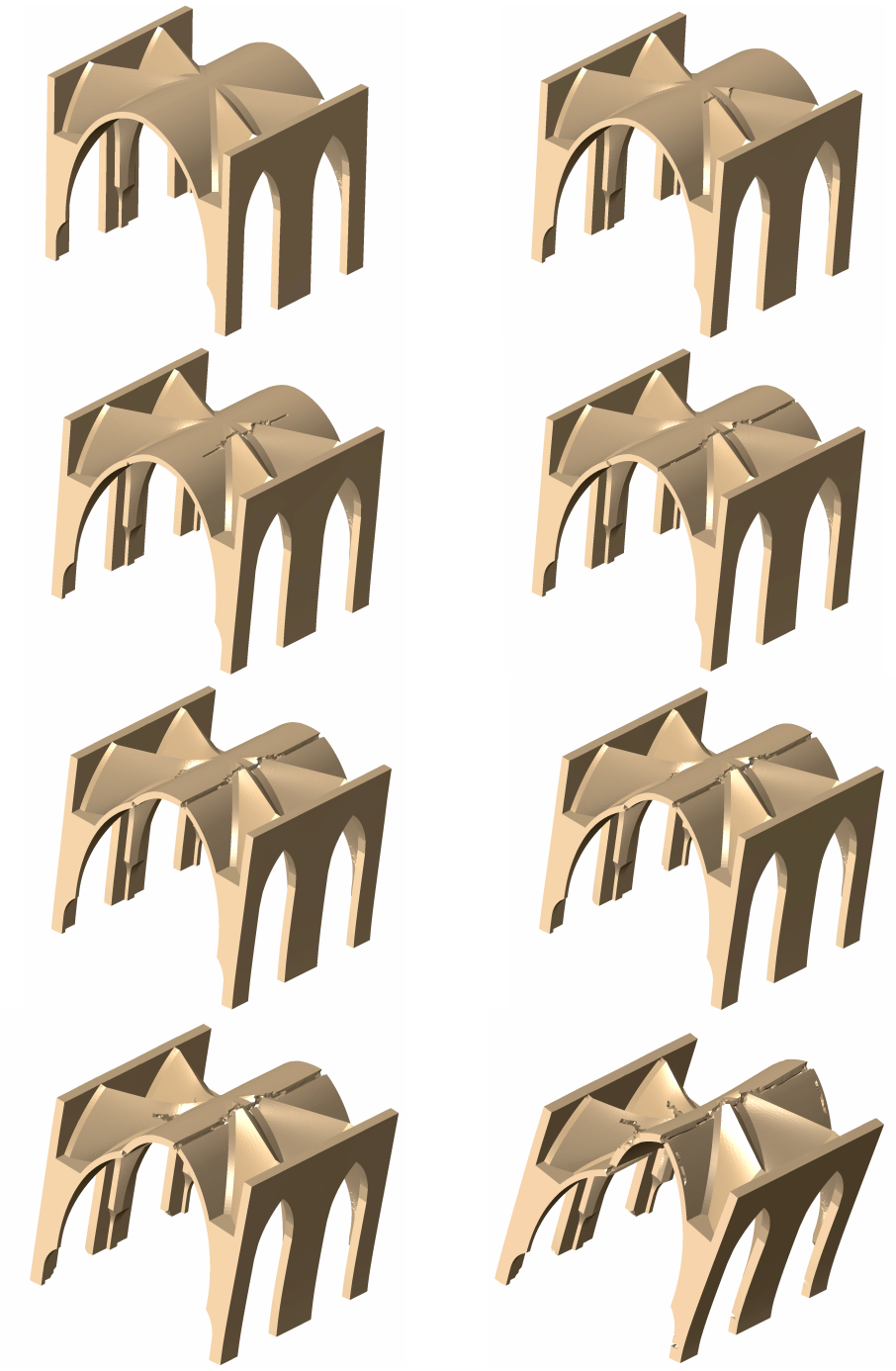

Figure 20: Progressive failure of the high sexpartite vault

Appendix A: numerical model convergence analysis

As the simulations are planned to be done by a two-step approach, see Sect. 5, we have validated the model using first a standard (implicit) scheme and then an explicit one. The response in both the cases has been evaluated on the eigenfrequencies of the first twenty vibration modes of the structure and on the vertical displacement of the keystone of the high vault, point V in Fig. 6, under the action of gravity.

The standard analysis is divided into two parts, namely a modal analysis and a static one with the gravity load. Both of these analyses have been made for eleven different meshes m, whose characteristics are given in Tab. 3.

Table 3: Characteristics of the studied meshes m.

m	Average element size $[m]$	Number of elements	Number of nodes
1	0.10	10616614	2101473
2	0.15	3432785	724257
3	0.20	1830092	406342
4	0.30	524967	130153
5	0.40	268222	70918
6	0.50	162751	45476
7	0.60	112388	32781
8	0.80	71952	21714
9	1.00	54474	16684
10	1.50	33396	10607
11	2.00	25827	8336

The first twenty eigenfrequencies f_m^j, $j = 1, 2, \ldots, 20$, and the vertical displacement of the point V of the sexpartite vault, u_m, are calculated for each mesh m. The convergence of the mesh has been evaluated calculating $\forall m$ the errors Δf_m^j of the frequencies f_m^j and Δu_m of the displacements u_m, relatively to the same quantities calculated for the reference mesh, the finest one, $m = 1$, having an average element size of 0.10 m:

$$\Delta f_m^j = \left| \frac{f_m^j - f_1^j}{f_1^j} \right|, \quad j = 1, 2, \ldots, 20, \qquad \Delta u_m = \left| \frac{u_m - u_1}{u_1} \right|. \tag{15}$$

In Fig. 21 we show the relative errors for the frequencies of the 1^{st}, 10^{th} and 20^{th} vibration modes of the structure along with that of the displacement of point V, in function of the number of elements of each mesh m.

A similar procedure was followed for investigating the mesh convergence for the explicit analysis. A mass proportional damping is applied in order to dissipate any oscillations due to the dynamic character of the analysis and to reach equilibrium faster. The convergence of the explicit analysis has been studied on the meshes $m = 2, 3, 11$, having an average element size of 0.15, 0.20 and 2.00 m respectively. The results are given in Tab. 4, where they are compared with the corresponding values of the standard (implicit) analysis. Also for the explicit analyses, the values of Δu_m have been normalized using eq. (15), i.e. using the value of $u_{m=1}$ calculated with the implicit scheme.

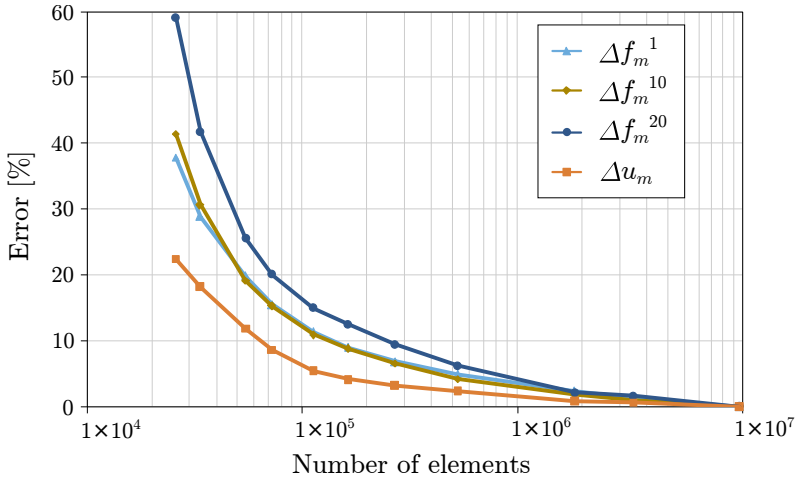

Figure 21: Relative error for three eigenfrequencies and the vertical displacement of point V as function of the elements number of each mesh m.

Table 4: Comparison of the relative errors for the vertical displacement of point V, calculated for three meshes with the implicit and explicit procedures.

m	Number of elements	Δu_m implicit [%]	Δu_m explicit [%]	Difference implicit-explicit [%]
2	3432785	0.64	0.28	0.36
3	1830092	0.84	0.36	0.48
11	25827	22.40	21.81	0.59

There are some very small differences between the explicit and the implicit analyses, to be imputed to some differences in the finite element formulation between the *ABAQUS Explicit* and *ABAQUS Standard* (implicit) solvers. Such differences are meaningless for the purpose of this study.

In Fig. 22 we show the total CPU time needed for the standard analyses in function of the number of elements, while in Fig. 23 we have plotted the same CPU time in function of the relative errors for the four quantities already represented in Fig. 21. In both the figures, the total CPU time is normalized with the CPU time of the finest mesh.

Looking at Figs. 21, 22 and 23, the choice of an average mesh size of 0.20 m seems a good balance between accuracy and calculation time. This is the mesh fineness that we have used in the calculations; as mentioned above, it has 1.83 millions of elements.

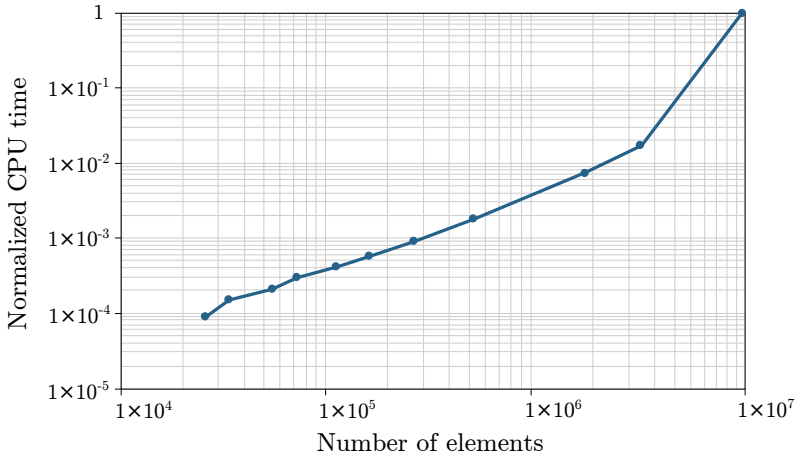

Figure 22: Normalized CPU times of the standard analyses versus the number of elements.

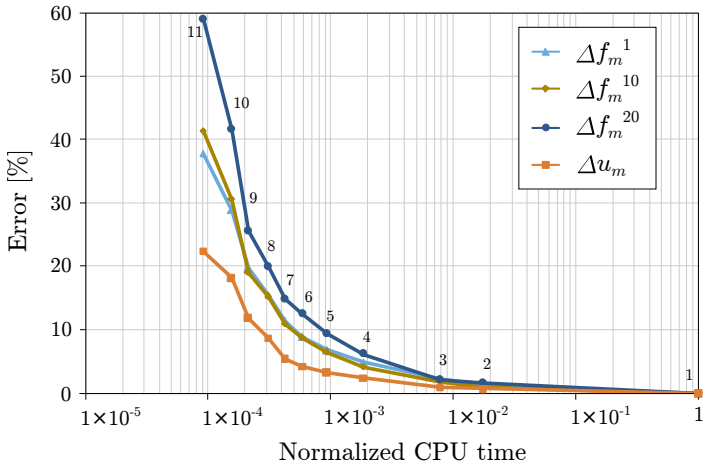

Figure 23: Normalized CPU times versus relative errors for three eigenfrequencies and the vertical displacement of point V; numbers 1 to 11 indicate the mesh m.

Appendix B: comparison of the wind profile with Eurocode 1

The European norms known as Eurocode are today the reference technical norms for civil constructions, not only in Europe. In particular, Eurocode 1 concerns the loads to be applied to structures and [ECS, 2005] is specific to wind loads. Conceived to be readily applied to standard situations of modern buildings to be designed and implicitly tuned to give, eventually, precise levels of structural safety, Eurocode 1 is not easily applicable to the case of a structure like Notre Dame of Paris. In fact, its shape can be hardly reduced to one of those considered in the norm and we are not concerned with a *design wind*, but we are looking for the strongest wind that the Cathedral can withstand.

In fact, our scope was not to design a structure according to a given code which includes several coefficients and parameters explicitly used for obtaining a standard safety, but to evaluate, as precisely as possible, the ultimate state of an *already existing structure* before failure under the wind thrust, considered as a static action (this assumption is justified by the fact that for a structure like a Gothic Cathedral, so massive, dynamic effects engendered by gusts can be neglected in regard of the global failure, though they can concern minor slender parts, like pinacles).

Anyway, it is interesting to compare our approach with the rules suggested by Eurocode 1 when adapted to the case of the Cathedral. This helps, on one hand, in shedding a new light on the use of such a code in cases like the present one and, on the other hand, in better evaluating the approach to the wind forces that we have followed in this work (largely inspired by the cited works [Mark, 1982] and [Coccia et al., 2015]).

For the case of Notre Dame of Paris, the wind profile according to Eurocode 1 is represented by a law of the type[1]

$$v(z) = \begin{cases} c_0(z_0)c_r(z_0)v_b & \text{if } z \le z_0, \\ c_0(z)c_r(z)v_b & \text{if } z > z_0, \end{cases} \tag{16}$$

where in the present case the two coefficients $c_0(z)$ and $c_r(z)$ are

$$c_0(z) = 1, \quad c_r(z) = 0.234 \ \ln z, \tag{17}$$

so finally

$$v(z) = \begin{cases} 0.539 \ v_b & \text{if } z \le z_0, \\ 0.234 \ \ln z \ v_b & \text{if } z > z_0. \end{cases} \tag{18}$$

In order to compare this wind profile with the one used in the paper, eq. (7), we need to put

$$v(z_0) = v_0 \to v_b = \frac{v_0}{0.234 \ \ln z_0} = 1.856 \ v_0, \tag{19}$$

so that, finally

$$v(z) = \begin{cases} v_0 & \text{if } z \le z_0, \\ 0.434 \ \ln z \ v_0 & \text{if } z > z_0, \end{cases} \tag{20}$$

and in the dimensionless form

$$\eta(z) = \begin{cases} 1 & \text{if } \zeta \le 1, \\ 1 + 0.434 \ln \zeta & \text{if } \zeta > 1. \end{cases} \tag{21}$$

The diagrams of eqs. (7) and (21) are plotted in Fig. 24; it is apparent that the two diagrams are so close that the differences are meaningless: the wind profile (7) gives an evaluation of the wind speed extremely similar to that proposed by Eurocode 1. Because eq. (7) tends toward zero for $z \to 0$, while eq. (21) tends towards $-\infty$, the power law is, in some sense, more physical than the logarithmic law proposed by Eurocode 1; anyway, this inconsistency of the norm if hidden by the assumed wind profile, constant from $z = 0$ to $z = z_0$.

For what concerns the drag coefficient C_D, Eurocode 1 specifies values that change from the windward to the leeward side and that vary with the height. Anyway, for the case of the Cathedral Notre Dame, the sum of the two drag coefficients is practically constant along the height, and equal to 1.5, the same value that we have used in the numerical simulations.

[1] Symbols used in this part are not necessarily those used by Eurocode 1, for having a more direct comparison with those used throughout the paper.

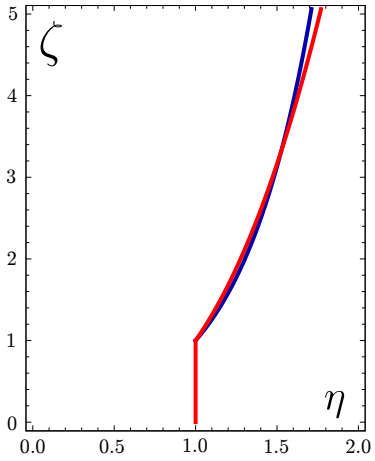

Figure 24: Comparison of the wind profiles given by power law (7), in red, and Eurocode 1, eq. (21), in blue.

References

A. Cecchi and K. Sab. A multi-parameter homogenization study for modeling elastic masonry. *European Journal of Mechanics - A/Solids*, 21:249–268, 2002.

N. Chien, Y. Feng, H. H. Want, and T. T. Siao. Wind tunnel studies of pressure distribution on elementary building forms. Technical report, Institute of Hydraulics Research, University of Iowa, Ames, Iowa, 1951.

S. Coccia, M. Como, and F. Di Carlo. Wind strength of Gothic Cathedrals. *Engineering Failure Analysis*, 55:1–25, 2015.

M. Como. *Statics of historic masonry constructions*. Springer Verlag, Berlin, Germany, 2013.

A. G. Davenport. The treatment of wind loads on tall buildings. In A. Coull and B. Stafford Smith, editors, *Tall Buildings*. Pergamon Press, New York, 1967.

ECS. Eurocode 1: Actions on structures — Part 1-4: General actions — Wind actions. Technical report, European Committee for Standardization, 2005.

P. Frankl. *Gothic architecture*. Pelican History of Art. Penguin Books, Baltimore, Maryland, 1963.

J. Heyman. *The stone skeleton*. Cambridge University Press, Cambridge, UK, 1995.

A. Hillerborg, M. Modéer, and P. E. Petersson. Analysis of crack formation and crack growth in concrete by means of fracture mechanics and finite elements. *Cement and Concrete Resistance*, 6:773–782, 1976.

H. Jantzen. *Kunst der Gotik*. Rowohlt Taschenbuch Verlag, Hamburg, Germany, 1957.

R. Mark. *Experiments in gothic structure*. MIT Press, Cambridge, Massachussets, 1982.

R. Mark. *High gothic structure - A technological reinterpretation*. Princeton University Press, Princeton, New Jersey, 1984.

P. Sachs. *Wind forces in engineering*. Pergamon Press, Oxford, UK, 1978.

O. Von Simson. *The Gothic Cathedral*. Princeton University Press, Princeton, New Jersey, 1962.

I. Stefanou, K. Sab, and J.-V. Heck. Three dimensional homogenization of masonry structures with building blocks of finite strength: A closed form strength domain. *International Journal of Solids and Structures*, 54:258–270, 2015.

A. Tallon. La Cathédrale de Paris, 2010. URL http://faculty.vassar.edu/antallon/ndp/vr/ndp_fr.html.

G. G. Ungewitter. *Lehrbuch der Gotischen Konstruktionen*. T. O. Weigel Nachfolger, Leipzig, Germany. Available at Biblioteca Meccanico Architettonica: http://www.bma.arch.unige.it, 1890.

R. van der Pluijm. *Out-of-Plane bending of Masonry. Behavior and Strength*. Technische Universiteit Eindhoven, Eindhoven, The Netherlands, 1999.

C. Wilson. *The Gothic Cathedral*. Thames & Hudson, London, UK, 1990.